

20030620027

Y P 11701
O P 2

AD-275 307

EXPLORATORY SAILWING RESEARCH AT PRINCETON

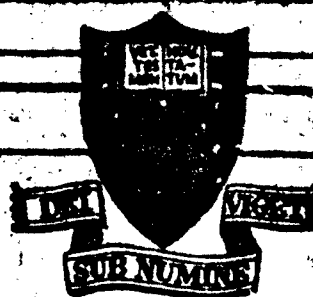
by

T. E. Sweeney

Department of Aeronautical Engineering
Princeton University

Report No. 578

December, 1961



PROPERTY OF U. S. ARMY
TRANSPORTATION RESEARCH COMMAND
RESEARCH REFERENCE CENTER

31 MAY 1962

PRINCETON UNIVERSITY
DEPARTMENT OF AERONAUTICAL ENGINEERING

Best Available Copy

U. S. Army Transportation Research Command
Fort Eustis, Virginia

Project Number: 9-38-10-000, TK⁰⁰²
Contract Number: DA44-177-72-524

EXPLORATORY SAILING RESEARCH AT PRINCETON

61-63
by

T. E. Sweeney

Department of Aeronautical Engineering
Princeton University

Report No. 578

December, 1961

Agencies within the Department
of Defense and their contractors
may obtain copies of this report
on a loan basis from:

Armed Services Technical
Information Agency
Arlington Hall Station
Arlington 12, Virginia

Others may obtain copies from:

Office of Technical Services
Acquisition Section
Department of Commerce
Washington 25, D. C.

The views contained in this
report are those of the contractor
and do not necessarily reflect
those of the Department of the
Army. The information contained
herein will not be used for
advertising purposes.

Approved by:

C. D. Perkins
C. D. Perkins, Chairman
Department of Aeronautical
Engineering, Princeton University

True ref 62-61

FOREWORD

Serious research looking into the Princeton Sailwing concept has been underway at Princeton University since early 1961 when it came under the sponsorship of the GEM Task Group, U. S. Army, TRECOM.

The original interest of the group was to determine the applicability of the sailwing as an auxiliary lifting device for a cruising ground effect machine. In order to make such a determination it was first necessary to explore the basic wing from the point of view of its structural and aerodynamic characteristics. The results of this initial exploratory work are presented in this report.

TABLE OF CONTENTS

	Page
I. Introduction	1
II. Discussion	
A. Models	2
B. Tests and Test Results	4
III. Conclusions	10
Appendix	11
Figures	
Distribution List	
Abstract Cards	

I. INTRODUCTION

The Princeton Sailwing, first conceived in 1948 as an advanced sail for a boat and later (in 1952) converted to a wing is shown schematically in Figure 1. It will be noted that the structure consists of a rigid leading edge and tip with a wire (in tension) trailing edge. The wing is ribless and is covered top and bottom with a flexible but ideally a non-stretchable fabric.

The original intent was to simplify, to a practical ultimate, a wing suitable for subsonic flight which would embody light weight, low cost, and easy foldability. It was not at first thought that such a wing would compare favorably with conventional hard wings. It will be seen, however, that there is considerable reason to expect that the aerodynamic efficiency of the sailwing can approach that of a hard wing.

The emerging facts from the study herein reported suggest that from all considerations the sailwing will find an important place in low speed aeronautics. The structural problems, while somewhat different from conventional practice, appear easily handlable. The deformations of the wing in flight seems to be in the direction of yielding reasonably high span efficiencies. The sailwing configuration as shown in Figure 1, seems to be compatible to almost any of the conventional planforms, whether they be swept, straight or tapered and with a wide range of aspect ratios. Sailwings so far tested have all been non-swept tapered wings of aspect ratios ranging from 6.0 to 14.0 yielding maximum lift coefficients as high as 1.7 with gentle stall characteristics. This is not to imply that there are no problem areas for, in fact, there are. These will be discussed in a later section.

II. DISCUSSION

A. Models

Since, at the outset of this exploratory research program, little was known of the behavior of sailwings it was decided to look at the most basic characteristics. This includes the following essential points to which answers were required for a preliminary evaluation of the concept:

1. The ballooning or deformation characteristics of the sail in forward flight.
2. The flutter behavior patterns of the wing in straight and yawed forward flight.
3. An estimate of the L/D characteristics.
4. The effect of porosity on the significant aerodynamic characteristics.
5. The effect of q and angle of attack on camber and thus performance.
6. The stall characteristics of the sailwing.
7. The practical aspects of a realistically sized sailwing.

In order to provide the necessary information for some understanding of the above unknown characteristics it was decided to construct several models - each one designed for a special purpose.

The first model - that of an aspect ratio 14 sailwing shown in Figures 2(a) and 2(b) was constructed and fitted to a go-cart to determine the gross effects of forward flight on the deformation and ballooning characteristics of the wing. It will be noted that both Figures 2(a) and 2(b) are essentially the same view of the wing - the former at rest while the second of these figures show the sail in forward motion at approximately ten degrees

angle of attack at 20 mph. In this figure the trailing edge deformation is clearly shown.

Figures 3(a) and 3(b) show the same aspect ratio 14 wing fitted to a model glider fuselage which was successfully flown approximately 50 times. This model was towed by auto and released when several feet in the air. The observations and measurements made with this craft will be discussed in the next section.

Figure 4 is a drawing of a two foot span, aspect ratio 6, taper ratio .33 sailwing designed for wing tunnel experiments. These tests were to determine the lift, drag, and pitching moment characteristics of such a configuration. It will be noted that, in this case, the leading edge is tubular with a piano wire trailing edge. This structure was covered with untreated aircraft fabric which is quite porous. As such it is considered to be the most primitive version of the sailwing. Figure 5 shows, pictorially, two views of this wind tunnel model. The results of these experiments are quite interesting and will be discussed in the next section. Of course, a major problem was how to extrapolate wind tunnel results to a full scale configuration. How to scale porosity is a problem seldom posed to subsonic investigators. This is, however, easily solved by testing a realistically sized model. Such a craft as pictured in Figure 6 was constructed mainly to determine C_L max, L/D and the C_L, α relationship of a useful size sailwing with minimum porosity. For this reason Dacron was selected as the sail material. It appears to be practically non-porous. To date, severe lateral control problems have limited the number of flights of this aircraft. The flights have, however, provided a rapid understand-

ing of the problems, solutions to which are presently underway. The detailed geometry of this glider is shown in Figure 7. It will be noted that the aspect ratio is 11.0 and that the planform is characterized by a concave trailing edge. This trailing edge configuration is required to keep a chordwise component of tension in the cloth covering material.

B. Tests and Test Results

The wings fitted to a Go-Cart shown in Figures 2(a) and 2(b) yielded the qualitative information that the sails do, indeed, deform in a quite predictable manner much as has been indicated in Figure 1. It had, at first, been feared that the upward deformation of the trailing edge wire, resulting in a reduction of angle of attack at mid-semispan would have a detrimental effect on span lift distribution. It is certainly so that the loading of the sail causes this loss in angle of attack. It is also so, however, that because of the chordwise lift at the least restrained location of the trailing edge wire (mid-semispan) that there is considerable deformation of the trailing edge wire in the forward direction. This is shown schematically in Figure 8. It will be noted in Figure 8 that as angle of attack is reduced due to vertical deformation in the trailing edge wire, considerable increase in camber is effected due to the forward deformation of the wire. The interesting results of this combined deformation is shown in Figure 9. This is a qualitative and quite idealized evaluation of the nature of the span lift distribution. It will be seen, from inspection of the Figure, that one might expect considerable deviation from the optimum elliptical lift distribution due to local angle of attack reduction in the vicinity of the mid-semispan. The effect of the camber increase in proportion to

angle of attack decrease, however, tends to wipe out this deviation from the ideal lift distribution yielding, in a general way, the results shown in Figure 9. In other words, the two effects are of a canceling nature. This, it is suspected, is one of the reasons why the sailing can, at some values of lift coefficient, compare so favorably in efficiency to a hard wing.

The original aspect ratio 14 wings fitted to the model glider fuselage (Figure 3) yielded the lift curve shown in Figure 10. The scatter in the data points in this Figure is the result of the very exploratory nature of the experiments. The model, as shown in Figure 3, was fitted with a tri-cycle landing gear, the nose wheel strut being adjustable in length. Thus, by varying the nose strut length, the ground angle of attack could be changed through approximately 20 degrees. The experiments consisted of measuring take-off velocity as a function of ground angle of attack. While the glider was trimable with an adjustable stabilizer it was not always possible to trim for a three wheel (zero rotation) take-off. This fact, more than any other, is responsible for the scatter of the data shown in Figure 10. Repeated experiments, however, statistically confirm the results shown.

The results of wind tunnel tests with the aspect ratio 6 model shown in Figure 4 appear in Figures 11 through 18. This model was first tested with the cotton cloth covering in its natural state. That is no treatment of the surface was made to reduce porosity or to increase strength. It was tested first remote from a ground board at two values of q and in ground effect ($h/\text{mac} = .45$) at the same two values of q . It will be noted in Figure 11 that the initial slope of the lift curve is increased as the

ground clearance is reduced. This is as would be expected and agrees in general to the behavior of hard wings near the ground.

More significantly, however, the initial slope of the lift curve even at $h/mac = \infty$ is extremely high for a three dimensional wing. Indeed, this value of $dC_L/d\alpha = .11$ rivals the slope of two dimensional lift curves. The explanation for this appears diagrammatically in Figure 12. This figure shows typical profiles of the model tested as a function of angle of attack. It will be noted that at $\alpha = 0^\circ$ the section is symmetrical. As angle of attack increases camber increases thus producing an effect on lift not unlike a hard wing with a geared flap (flap deflection mechanically related to angle of attack).

The Figures 13(a) and 13(b) show the drag characteristics of this model. It is emphasized that the values of drag coefficient shown are artificially high. They are taken from data not corrected for tare. It will be noted in Figure 13(a) that drag increases with q , probably due to the greater leakage through the porous cloth. Figure 13(b) indicates little or no change in drag with change in h/mac . This is also in agreement with the general behavior of hard wings in and out of ground effect.

Figures 14(a) and 14(b) show the general stability characteristics of the untreated cloth wing - first under the conditions of variable q and constant h/mac and also for constant q with variable h/mac . The most interesting observation to be made from these results is the strong longitudinal stability of the wing. It is deduced that this is also an effect of the variable camber characteristic of the wing. It will be noted that each of the stability curves tend to break at a value of lift coefficient of approximately .3 to a somewhat less stable slope but still retaining unusually

good stability up to the stall. In general there seems to be little effect of q on the slope of the pitching moment curve but there is a pronounced effect of ground effect upon this slope. This effect of close proximity to the ground of significantly increasing longitudinal stability is in agreement with the general behavior of hard wings in ground effect.

Upon completion of the wind tunnel tests with the porous model an attempt was made to decrease the porosity by impregnating the cloth with a light wax. The results of repeat experiments utilizing the treated model appear in Figures 15 and 16. It will be noted in Figure 15 that the initial slope, a_0 , of the lift curve, while still extremely high for an aspect ratio 6 wing, is slightly lower than that for the untreated wing. The reason for this appears to be because the waxed wing was substantially stiffer than the non-waxed surface thereby somewhat restricting the camber change with angle of attack.

Figure 16 shows that the drag characteristics are considerably improved by decreasing the porosity of the cloth. Again it is emphasized that these are not absolute values of wing drag but include high tare drags.

In an attempt to arrive at a close approximation of the lift/drag characteristics of the sailwing it was decided to test an existing hard model of a Navion wing in the same tunnel using the same balance and velocities that were used for the sailwing experiments. The results of these Navion wing tests allowed not only a direct comparison with sailwing results, but also permitted a reasonable method of closely estimating tunnel drag tares since Navion wing characteristics are well known. Such a comparison appears valid, chiefly because the two models had the same aspect ratio, span and

area. Therefore the wind tunnel wall and horizontal buoyancy effects should be identical.

The results of the corrected drag measurements are shown in Figure 17 for both the Navion wing and the aspect ratio 6, untreated sailwing. Figure 17(a) compares the sailwing and Navion wing polars showing a tendency toward convergence at the higher values of lift coefficient. This is also shown in terms of L/D versus C_L in Figure 17(b). The sailwing tested appears to have a maximum L/D of approximately 11.0 occurring at a lift coefficient of .4. It should be emphasized that this L/D max. of 11.0 is for the untreated cotton cloth wing and is thus the most unsophisticated version of the concept. The final comparison of the two wings is made in Figure 18 which shows directly the relative L/D ratios in terms of an effective efficiency versus lift coefficient.

The third sailwing model from which observations and data have been obtained is the man-carrying sailwing glider. This machine is shown in Figures 6 and 7. Unlike the tubular leading edge of the wind tunnel model this sailwing has a drooped symmetrical D-spar leading edge which is hinged and readily foldable.

The reason for the drooped leading edge is shown in Figure 19. It will be noted in the top diagram of Figure 19 that the non-drooped leading edge (as used on the 12' free flight model glider) causes a discontinuity of the lower surface. Since such a sharp break in the camber is drag producing it is advantageous to eliminate it. Of the several means of accomplishing a smoother camber (including a transition fairing as shown in Figure 19) the drooped spar was selected for the full scale wing. The sail

is 3.8 oz. Dacron which was selected for its dimensional stability (non-stretchability) and for its lack of porosity. Figure 20 shows the wing structure folded prior to the attachment of the sail. Pertinent specifications for this sailwing glider are as follows:

Span	= 30'
Length	= 19'
Height	= 6.75'
Area	= 88 ft. ²
W/S	= 5.5 #/ft. ²
Aspect Ratio	= 11.0
C _L max.	= 1.7
Weight (with Pilot)	= 480 lbs.

The original purpose of this machine was to determine the C_L, curve and the L/D, C_L curve for a realistically sized sailwing. In addition, much valuable qualitative information has been gained including such important observations as the nature of the camber distribution and the extent to which flutter is a problem. To date, eight flights have been made testing different methods of lateral control. The wing has performed in a quite predictable manner even during a full stall landing. It will be noted in Figure 6 that the sail is made up of a number of alternate colored Dacron Strips. This color pattern permits a visual and photographic interpretation of the camber. Figures 21 and 22 show the under-camber and upper camber when the glider is in forward motion just prior to take-off. Research flights are continuing with this machine, the results of which, will, it is hoped, permit the next generation sailwing craft to be a useful powered airplane of extreme simplicity, light weight, with foldable wings of relatively high efficiency.

III. CONCLUSIONS

From the numerous experiments herein reported certain conclusions can be drawn:

1. The Princeton Sailwing does deform in a generally predictable manner.
2. The deformation of the wing produces a loss in angle of attack at the mid-semispan region but tends to cancel this detriment to efficient span lift distribution by an increase in camber in this region.
3. For the reason mentioned above the ultimate efficiency of a sailwing can approach that of a good hard wing.
4. The sailwing is easily foldable, light in weight and low in cost.
5. The initial slope of a sailwing lift curve is very high by three dimensional standards and the wing is very stable longitudinally. Both of these characteristics seem to be due to the camber change with angle of attack.
6. It is most important from the point of view of low drag to have a non-porous sail. Dacron appears to be an excellent material for this application.
7. The stall characteristics of the wing appear gentle. Wind tunnel tests indicate this and full scale test flights have confirmed this stall characteristic.
8. Within the limits of the full scale Reynolds Numbers so far encountered (1.5×10^6) wing flutter or excessive wrinkling does not seem to be a problem.

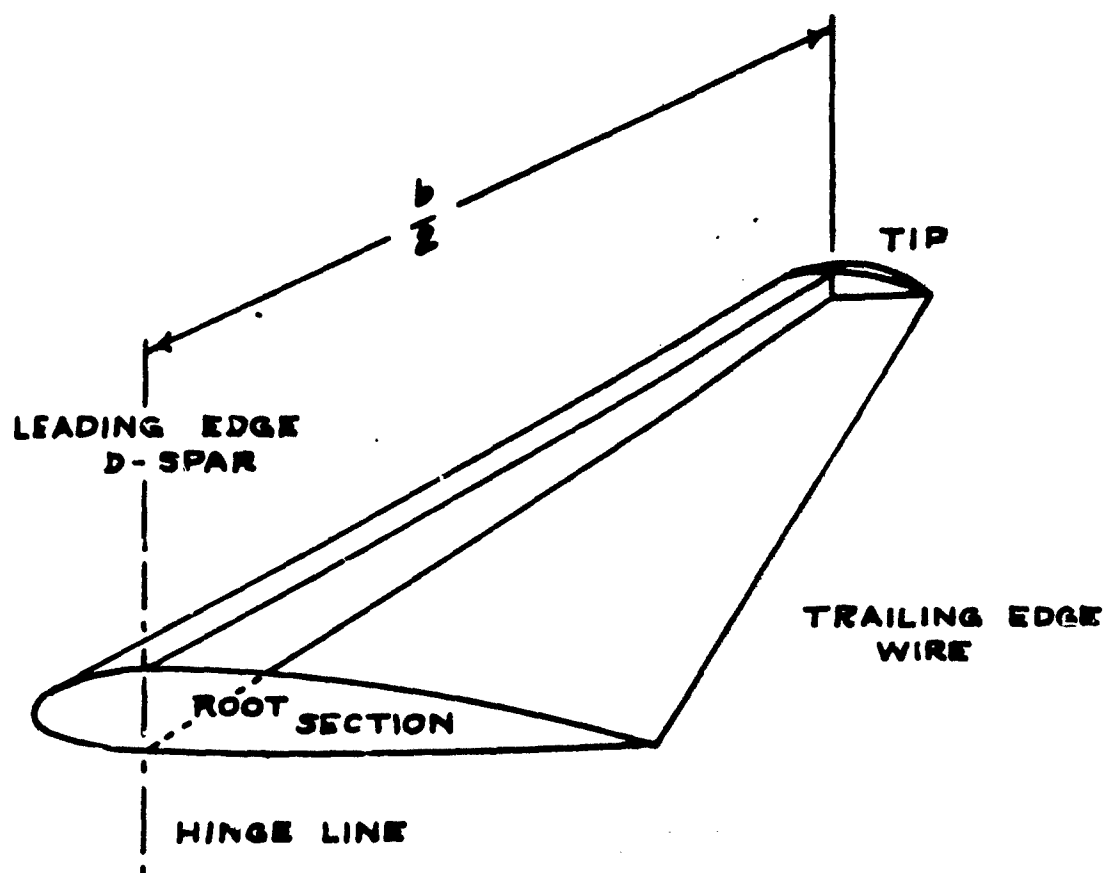
APPENDIX

As mentioned in the foreword, work with the Princeton Sailwing concept was undertaken and sponsored by the GEM Task Group, TRECOM to determine the feasibility of sailwings as an auxiliary lifting device for ground effect machines.

It is the author's considered opinion that sailwings are ideally suited to such an application for the type of GEM intended to cruise at relatively high speed over reasonable rough surfaces (particularly water) with efficiencies not ordinarily associated with ground effect machines. This opinion is based upon the promise of high L/D ratios particularly at high lift coefficients when in close proximity to the ground. The easy foldability and deployability is another valuable asset of the concept - not only for GEM application but for some aircraft uses as well.

BASIC SAILWING STRUCTURE

FIG. 1



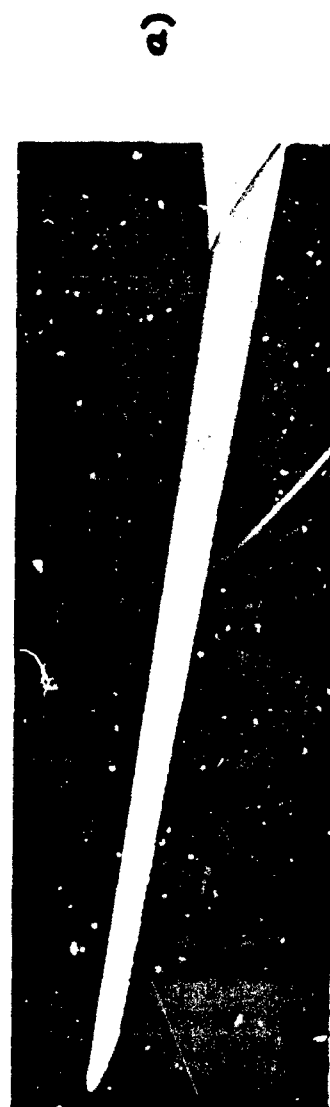
STRUCTURE COVERED TOP AND BOTTOM
WITH FLEXIBLE CLOTH

TYPICAL
SECTIONS

UNLOADED
(AT REST)

LOADED
(FORWARD
FLIGHT)

FIG. 2



AT REST



FORWARD
MOTION
V = 25 MPH

TRAILING EDGE VIEWS , ASPECT RATIO .4 SAILWING

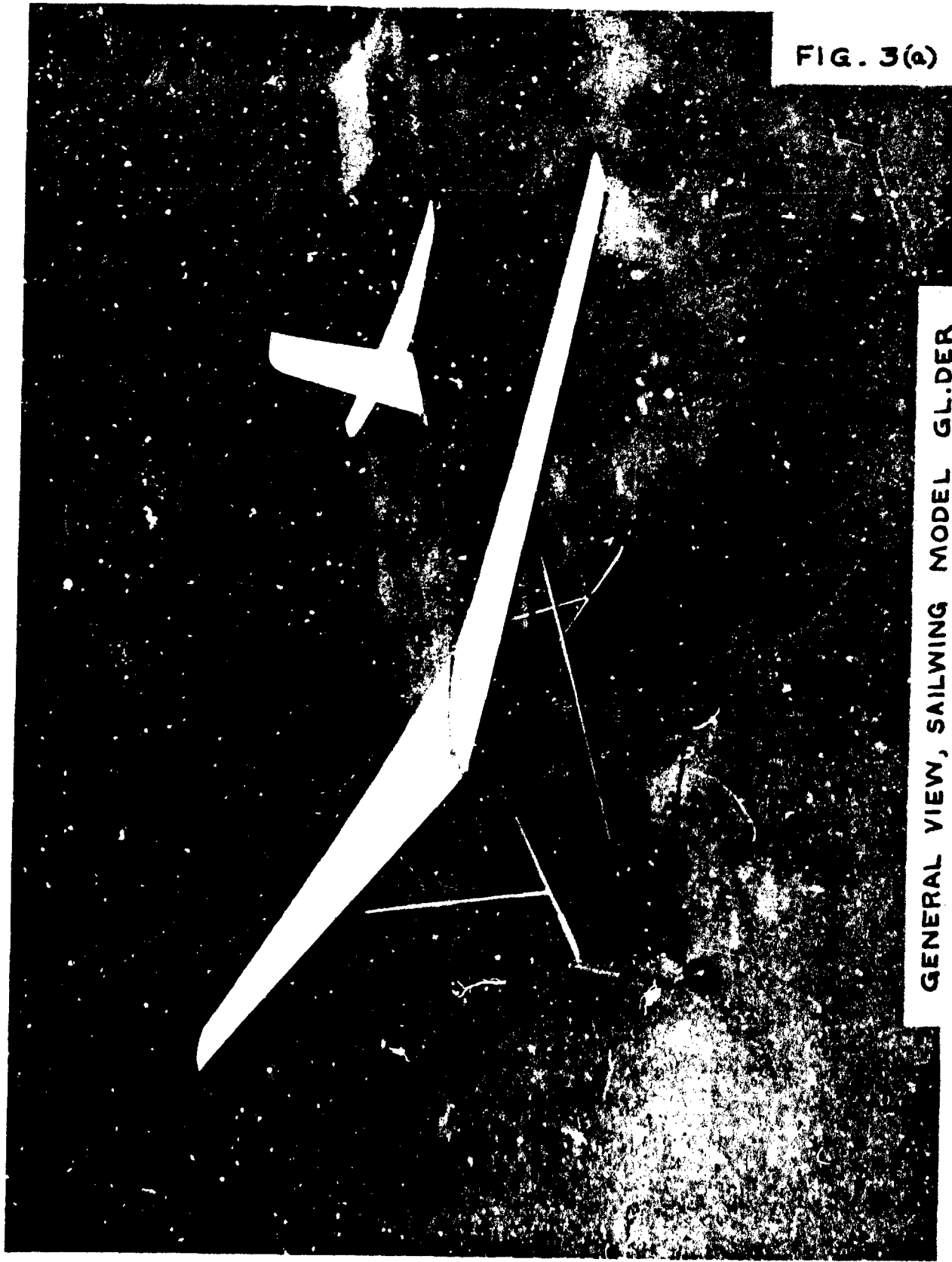


FIG. 3(a)

GENERAL VIEW, SAILWING MODEL GLIDER

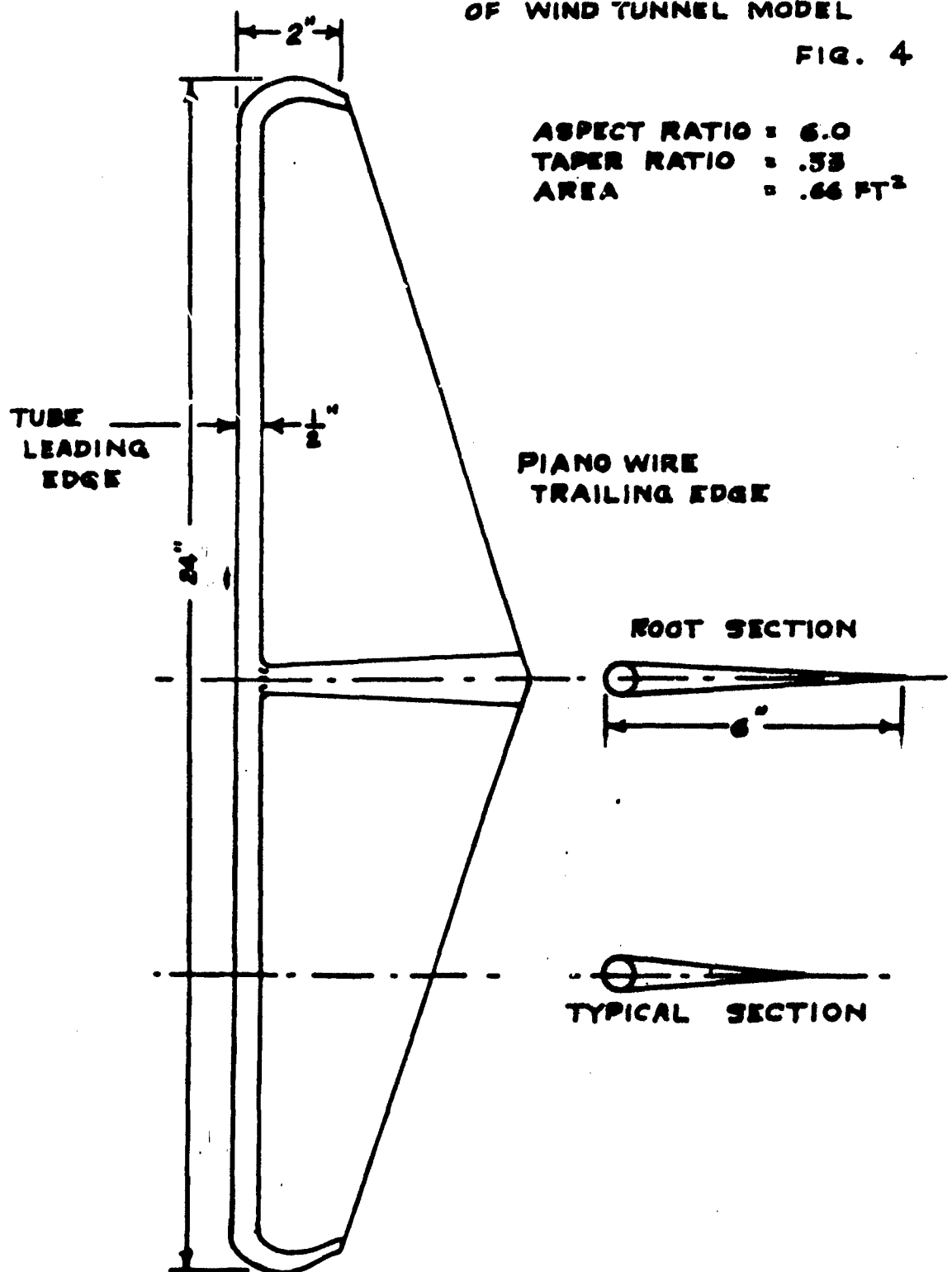
FIG. 36



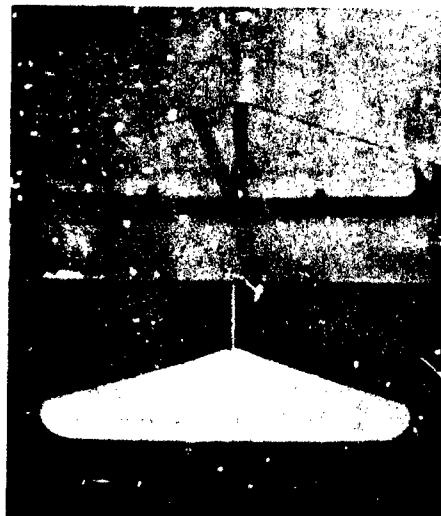
MAJOR GEOMETRIC CHARACTERISTICS
OF WIND TUNNEL MODEL

FIG. 4

ASPECT RATIO = 6.0
TAPER RATIO = .53
AREA = .66 FT²



TWO VIEWS OF WIND TUNNEL MODEL FIG. 5
SAILWING



BEFORE
COVERING

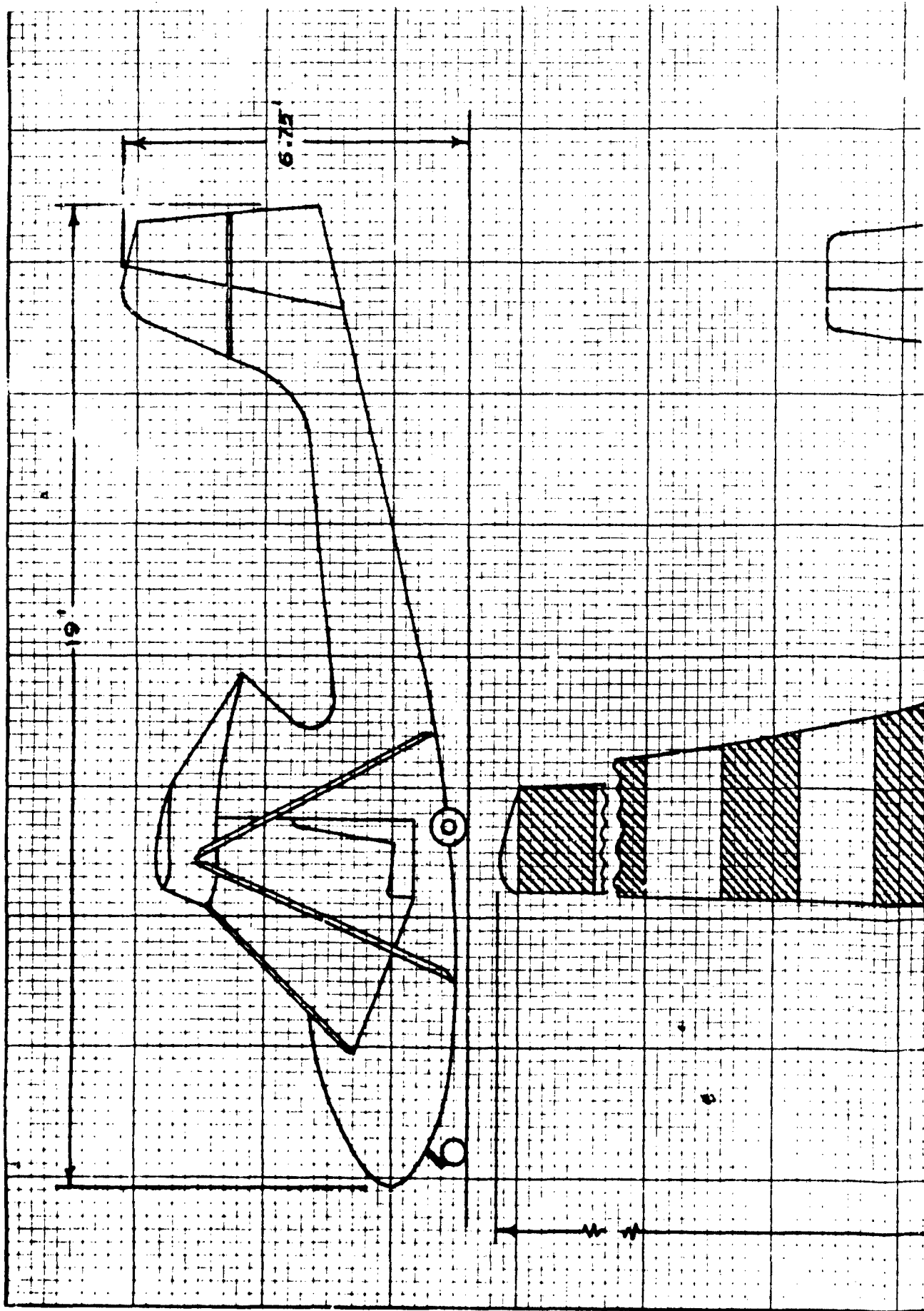
AFTER
COVERING

ASPECT RATIO 6.0
TAPER RATIO .33



FIG. 6

GENERAL VIEW OF FULL-SCALE SAILWING

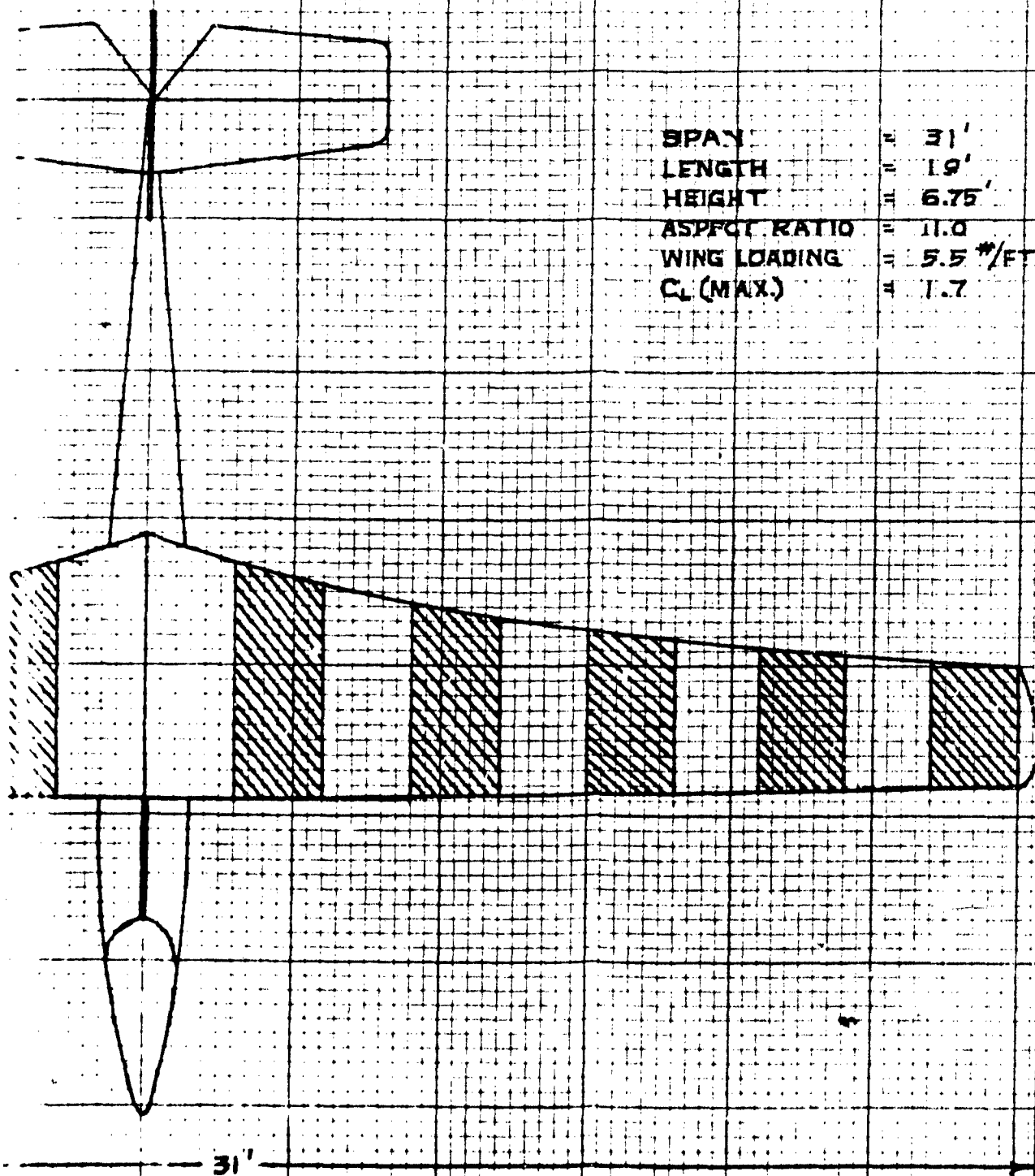


①

FIG. 7

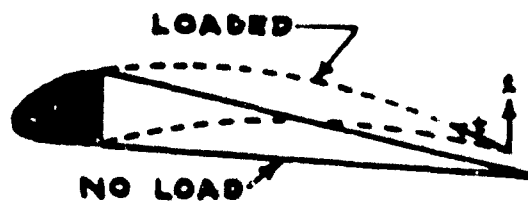
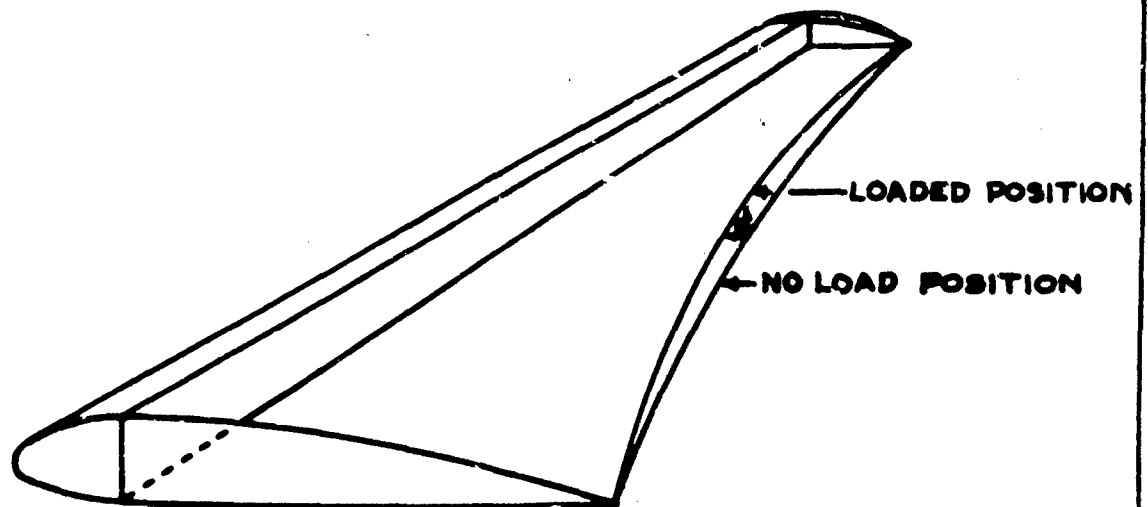
GENERAL LAYOUT AND
PRINCIPAL DIMENSIONS
OF
SAILWING II

SPAN	= 31'
LENGTH	= 19'
HEIGHT	= 6.75'
ASPECT RATIO	= 11.0
WING LOADING	= 5.5 #/FT ²
C _L (MAX.)	= 1.7



**BEHAVIOR OF TRAILING EDGE WIRE WITH
APPLICATION OF LOAD**

FIG. 8



**T. E. WIRE
DEFORMED UP-
WARD DUE TO
LIFT AND FOR-
WARD DUE TO
CHORDWISE
TENSION IN
CLOTH**

QUALITATIVE NATURE OF SAILWING SPAN LIFT DISTRIBUTION

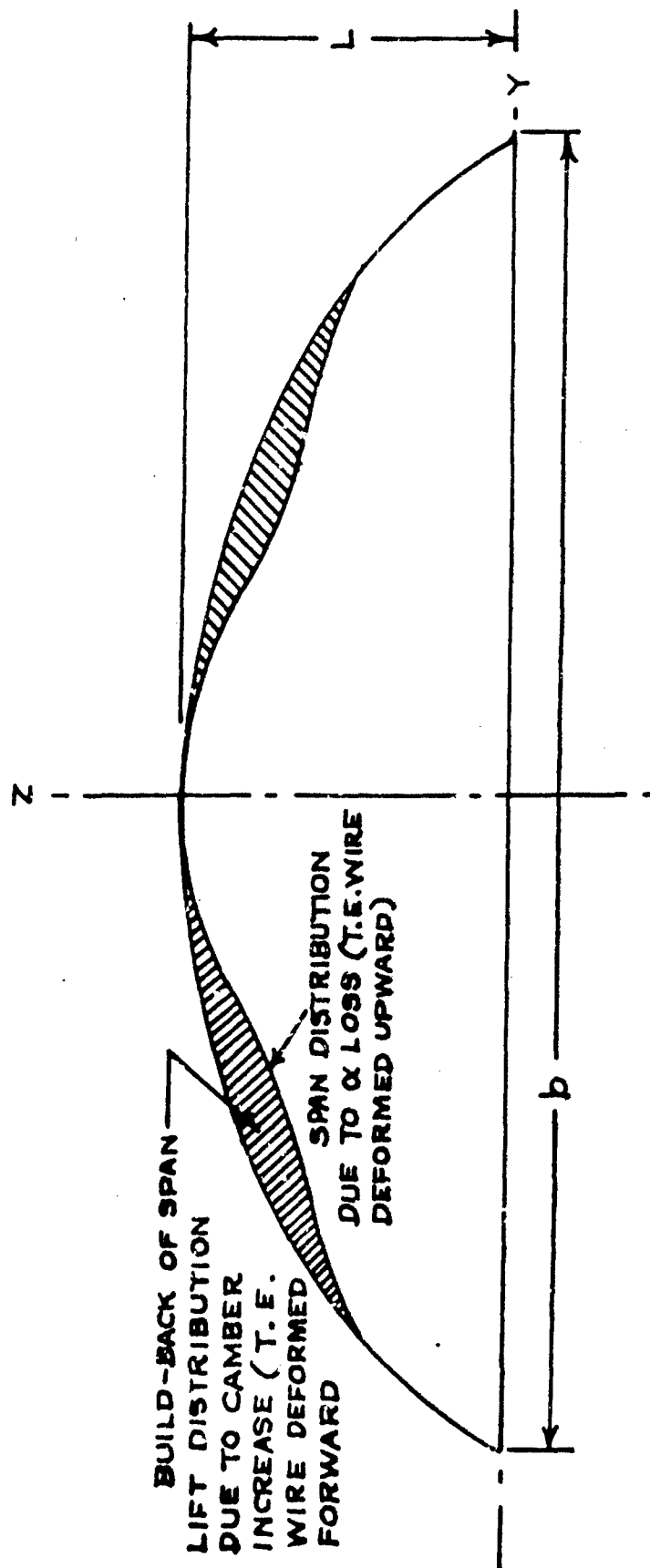
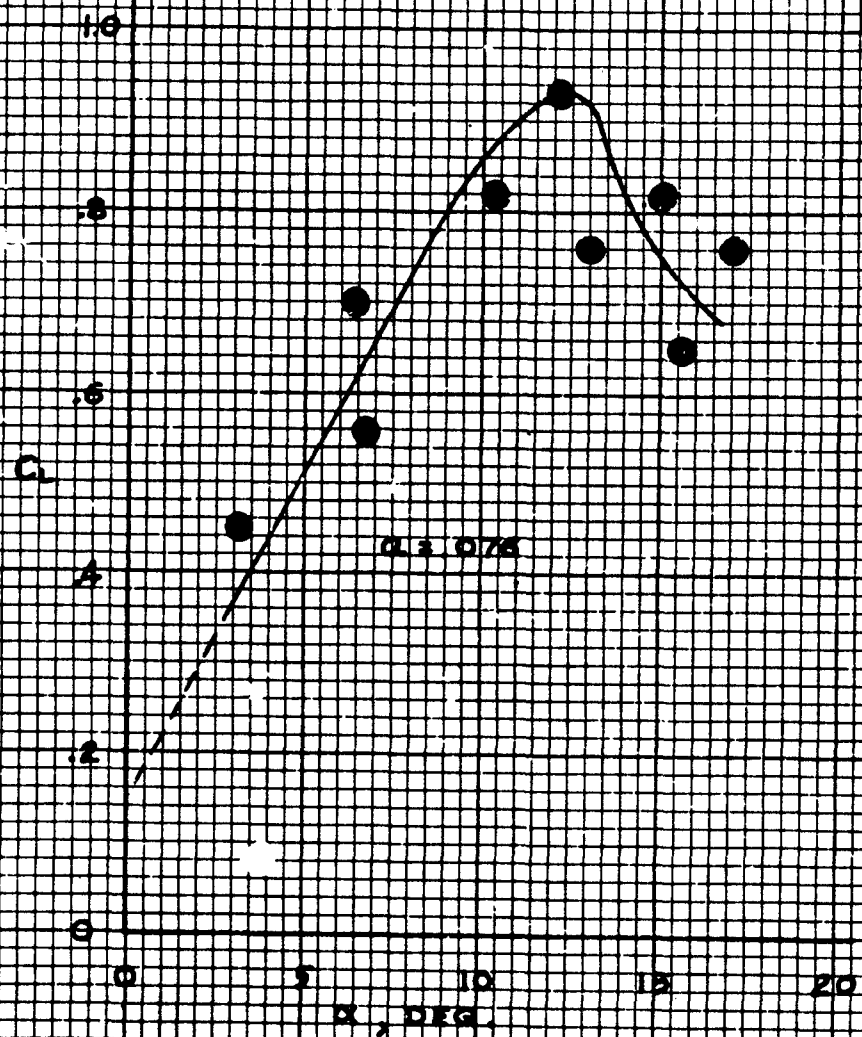


FIG. 9

LIFT COEFFICIENT VERSUS ANGLE OF ATTACK SAILWING I - FREE FLIGHT GLIDER

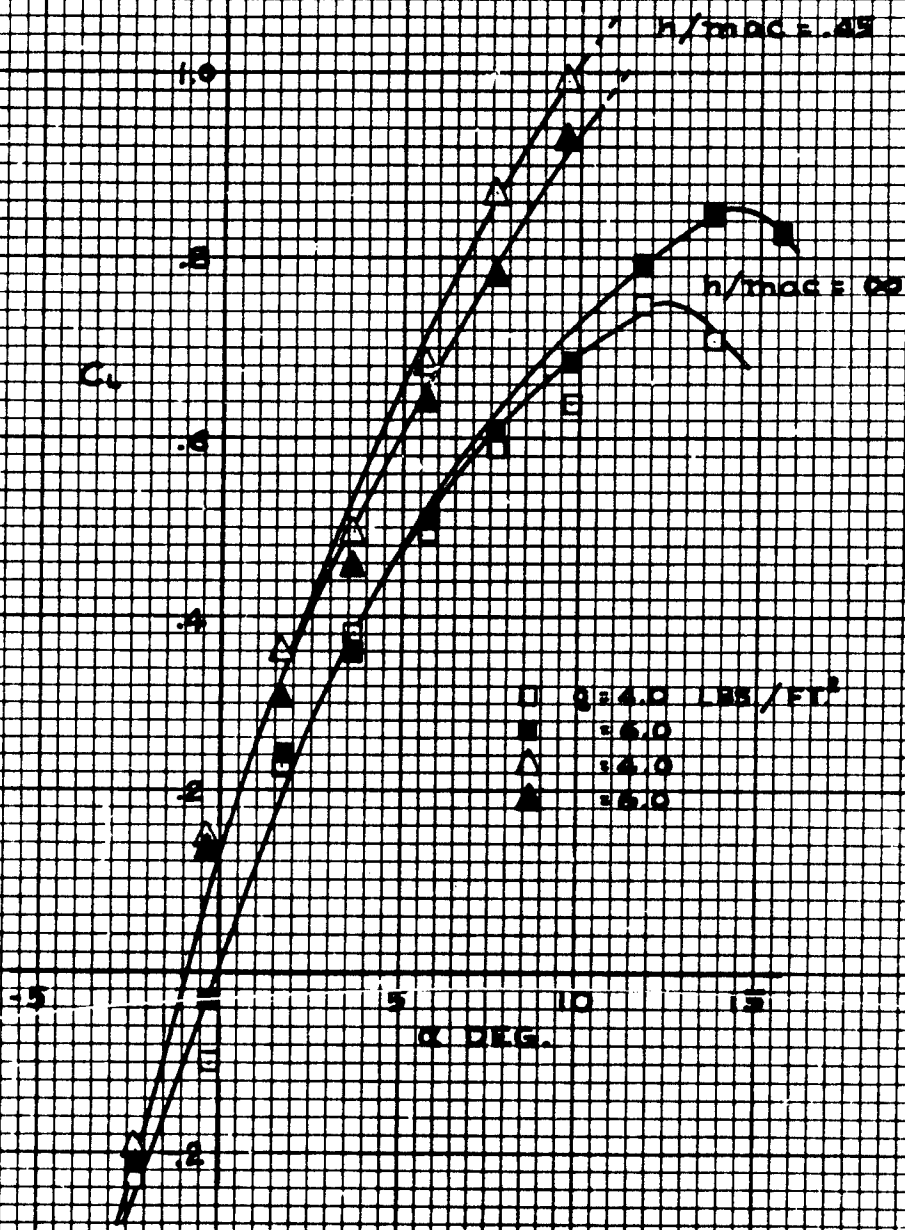
FIG. 1



ASPECT RATIO 6, TAPER RATIO .33 SAILING
LIFT CHARACTERISTICS AS A FUNCTION OF q AND h/mac

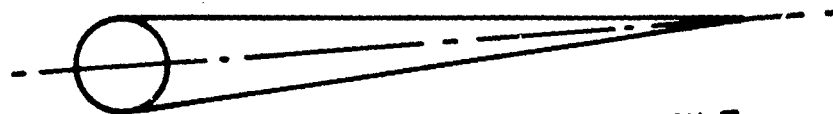
FIG. III

UNTREATED COTTON DUCK SAIL

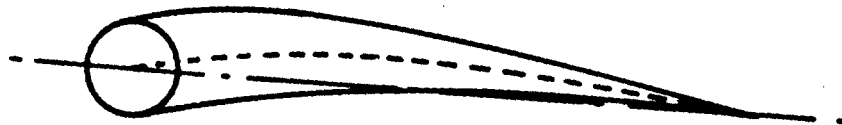


QUALITATIVE BEHAVIOR OF
CAMBER CHANGE WITH ANGLE OF ATTACK

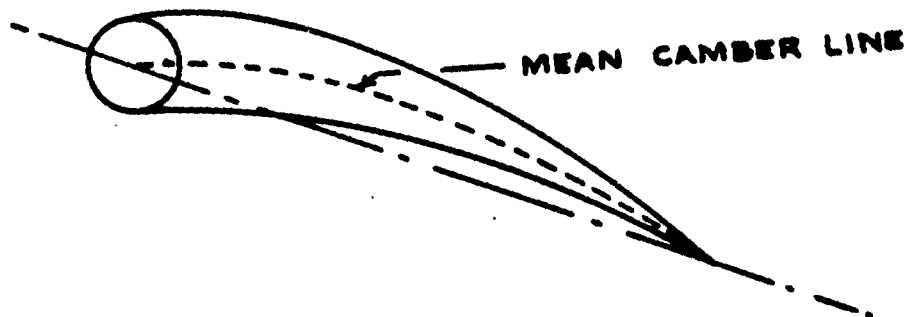
FIG. 12



$\alpha = 0^\circ$ ~ SYMMETRICAL PROFILE



$\alpha = +^\circ$ ~ MODERATE CAMBER
PROFILE

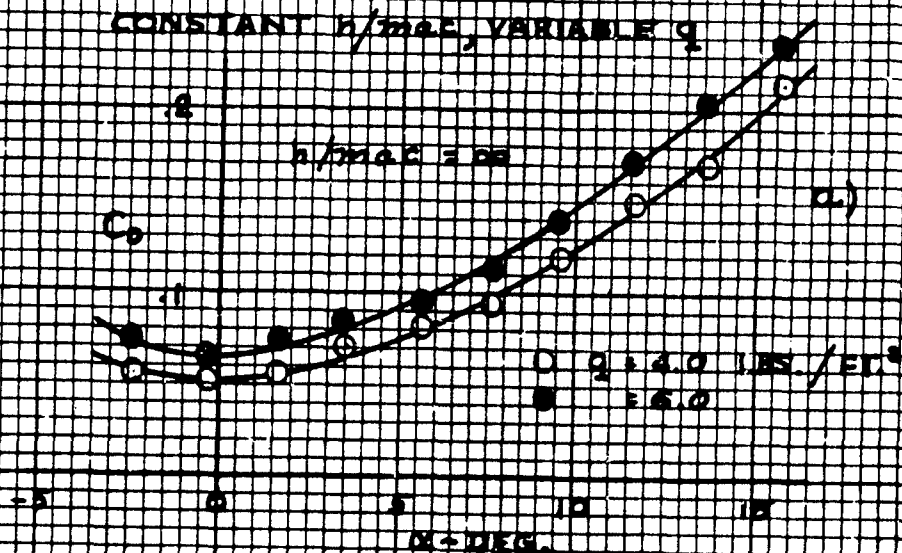


$\alpha = ++^\circ$ ~ HIGHLY CAMBERED
PROFILE

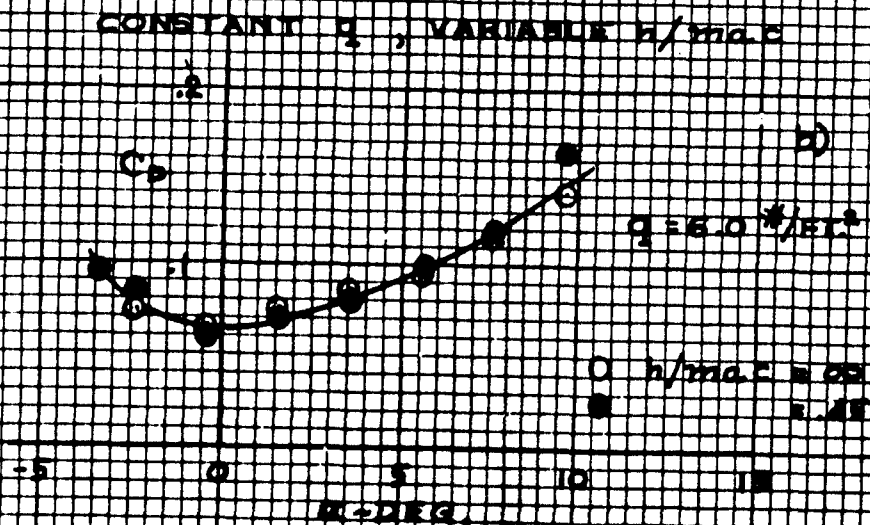
ASPECT RATIO 5, TAPER RATIO .33 SAILING
DRAG CHARACTERISTICS AS A FUNCTION OF q AND h/mac

FIG. 13

UNTREATED COTTON DUCK SAILS



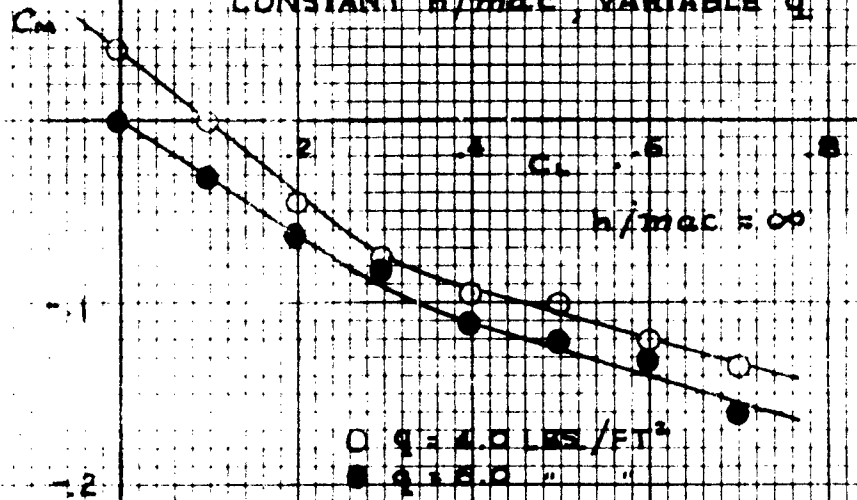
NOTE: DRAG NOT CORRECTED
FOR TARES



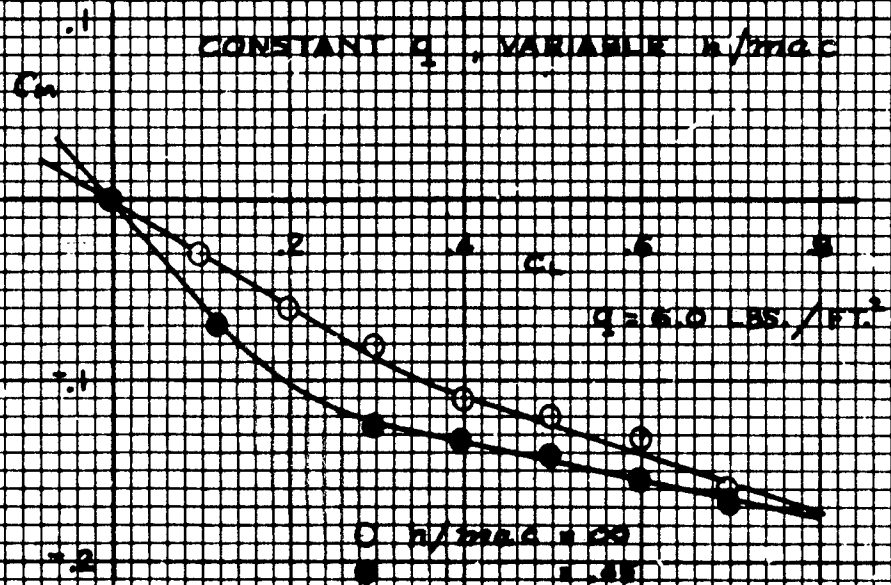
ASPECT RATIO 5, TAPER RATIO .33 SAILWING
STABILITY CHARACTERISTICS AS A FUNCTION OF q AND h/mac
UNTREATED COTTON DUCK SAILS

FIG. 14

CONSTANT h/mac , VARIABLE q



CONSTANT q , VARIABLE h/mac

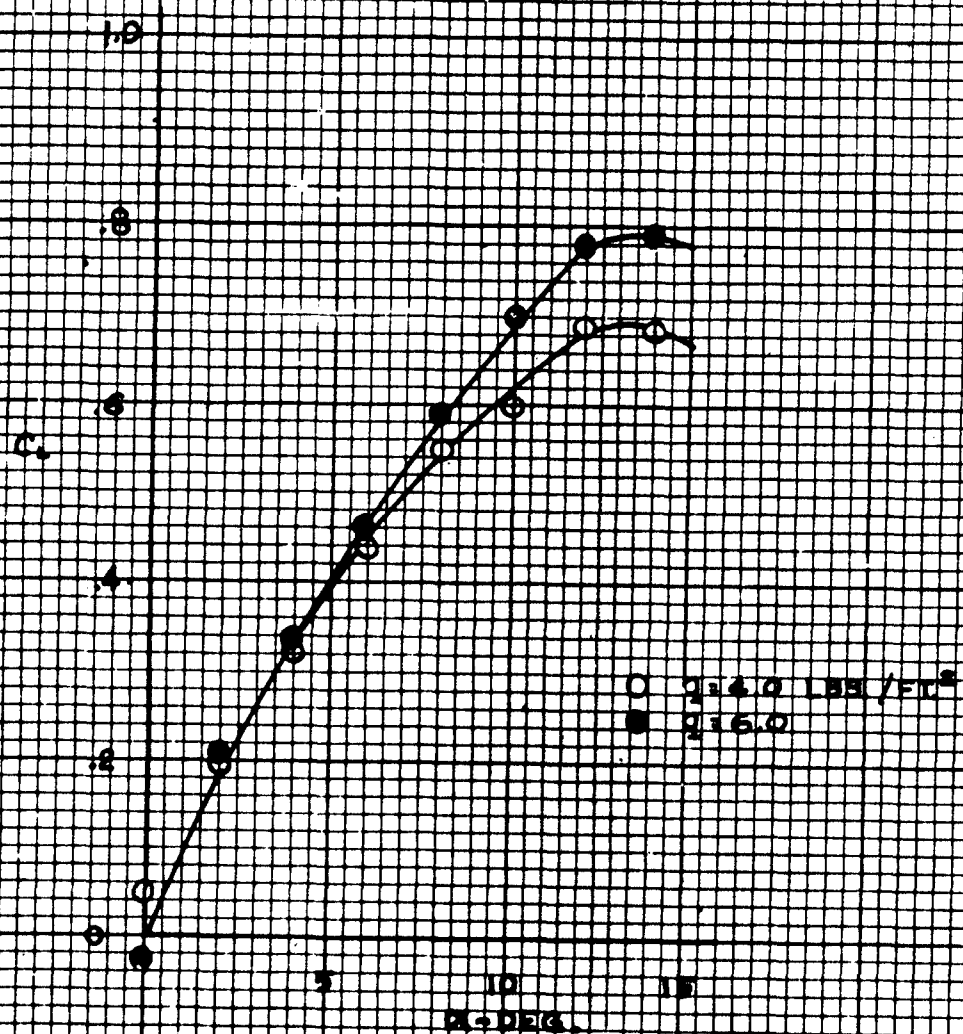


ASPECT RATIO 6, TAPER RATIO .33 SAILWING
LIFT CHARACTERISTICS AS A FUNCTION OF q LBS./FT.

$$h/w_{\text{tip}} = .60$$

FIG. 13

TREATED COTTON DUCK SAILS

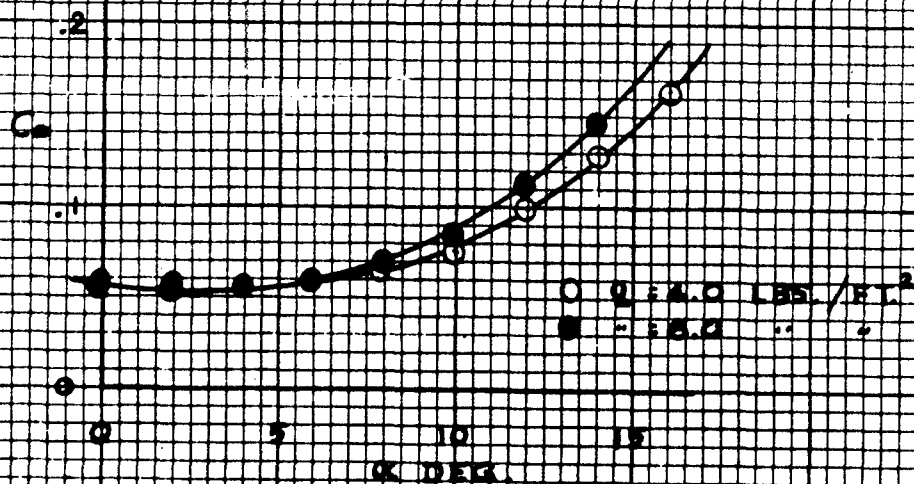


ASPECT RATIO 6, TAPER RATIO .33 SAILWING
 DRAG CHARACTERISTICS AS A FUNCTION OF Q

$$h / \pi a c = .60$$

FIG. 15

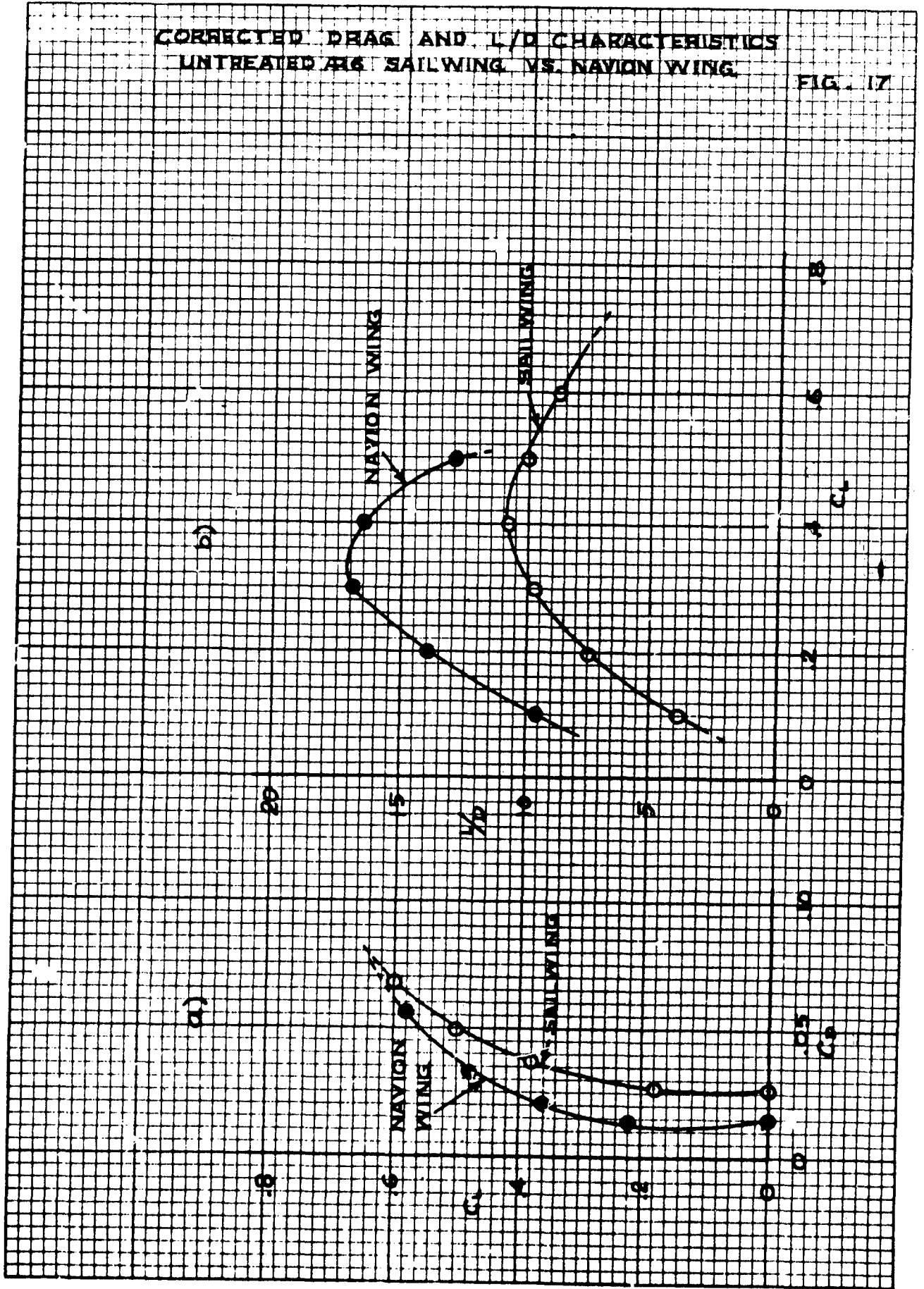
TREATED COTTON DUCK SAILS



NOTE: DRAG NOT CORRECTED FOR TARES

CORRECTED DRAG AND L/D CHARACTERISTICS UNTREATED AR6 SAIL WING VS. NAVION WING

FIG. 17



COMPARISON OF SAILWING AND NAVION WING PERFORMANCE A6 UNTREATED SAILWING

FIG. 18

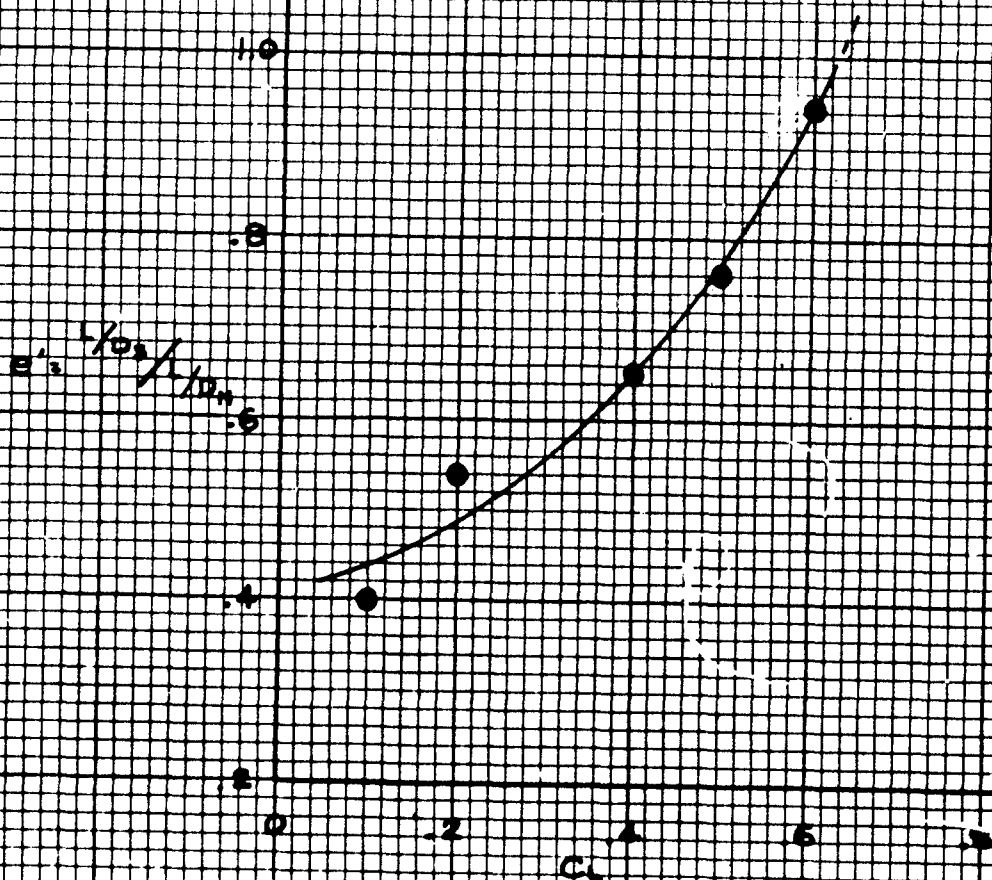


FIG. 19

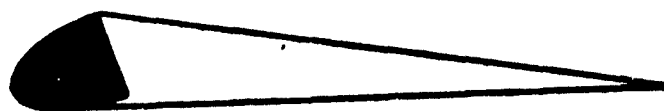
NON-DROOPED SPAR PROFILE (LOADED)



NON-DROOPED SPAR PROFILE (LOADED)



DROOPED SPAR (UNLOADED)



DROOPED SPAR PROFILE (LOADED)



FIG. 20



FULL SCALE SAILWING, SPAR IN FOLDED POSITION

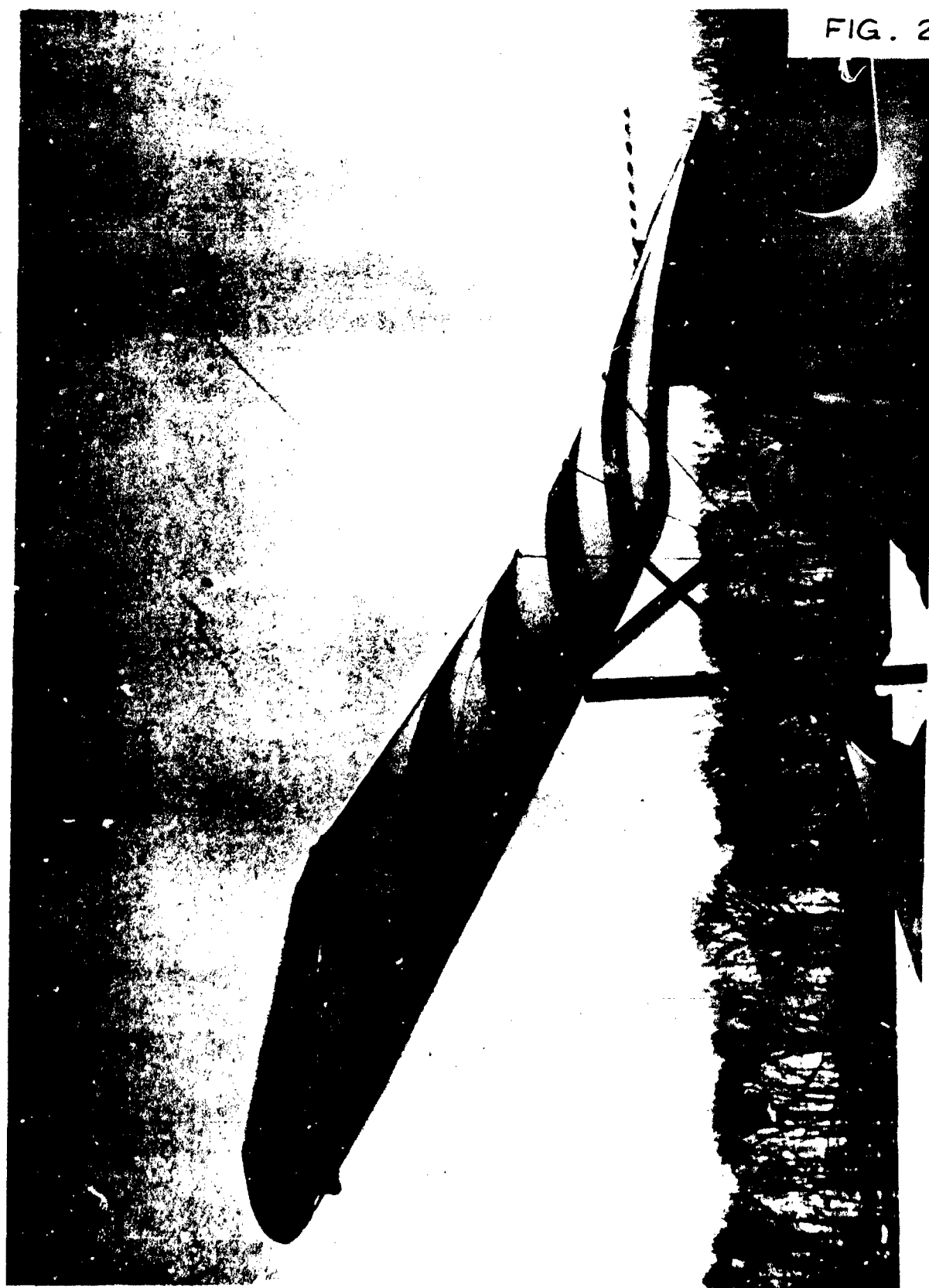


FIG. 21

VIEW OF SAILWING UNDER-CAMBER DISTRIBUTION

FIG. 22



VIEW OF SAILWING UPPER - CAMBER

ALART PROGRAM
Technical Report
Distribution List

ADDRESS	NO. OF COPIES
1. Chief of Transportation Department of the Army Washington 25, D. C. ATTN: TCACR	(2)
2. Commander Wright Air Development Division Wright-Patterson Air Force Base, Ohio ATTN: WCLJA	(2)
3. Commanding Officer U. S. Army Transportation Research Command Fort Eustis, Virginia ATTN: Research Reference Center ATTN: Aviation Directorate	(4) (3)
4. U. S. Army Representative HQ AFSC (SCR-LA) Andrews Air Force Base Washington 25, D. C.	(1)
5. Director Air University Library ATTN: AUL-8680 Maxwell Air Force Base, Alabama	(1)
6. Commanding Officer David Taylor Model Basin Aerodynamics Laboratory Washington 7, D. C.	(1)
7. Chief Bureau of Naval Weapons Department of the Navy Washington 25, D. C. ATTN: Airframe Design Division ATTN: Aircraft Division ATTN: Research Division	(1) (1) (1)

ADDRESS	NO. OF COPIES
8. Chief of Naval Research Code 461 Washington 25, D. C. ATTN: ALO	(1)
9. Director of Defense Research and Development Room 3E - 1065, The Pentagon Washington 25, D. C. ATTN: Technical Library	(1)
10. U. S. Army Standardization Group, U. K. Box 65, U. S. Navy 100 FPO New York, New York	(1)
11. National Aeronautics and Space Administration 1520 H Street, N. W. Washington 25, D. C. ATTN: Bertram A. Mulcahy Director of Technical Information	(5)
12. Librarian Langley Research Center National Aeronautics & Space Administration Langley Field, Virginia	(1)
13. Ames Research Center National Aeronautics and Space Agency Moffett Field, California ATTN: Library	(1)
14. Armed Services Technical Information Agency Arlington Hall Station Arlington 12, Virginia	(10)
15. Office of Chief of Research and Development Department of the Army Washington 25, D. C. ATTN: Mobility Division	(1)
16. Senior Standardization Representative U. S. Army Standardization Group, Canada c/o Director of Weapons and Development Army Headquarters Ottawa, Canada	(1)

	ADDRESS	NO. OF COPIES
17.	Canadian Liaison Officer U. S. Army Transportation School Fort Eustis, Virginia	(3)
18.	British Joint Services Mission (Army Staff) DAQMG (Mov & Tn) 1800 "K" Street, NW Washington 6, D. C. ATTN: Lt. Col. R. J. Wade, RE	(3)
19.	Office Chief of Research and Development Army Research Office ATTN: Physical Sciences Division Arlington Hall Station Washington 25, D. C.	(2)
20.	Librarian Institute of the Aeronautical Sciences 2 East 64th Street New York 21, New York	(2)
21.	Chief US Army Research and Development Group (Europe) ATTN: USATRECOM Liaison Officer APO 757 New York, New York	(1)

This report describes the structure and the dominant aerodynamic characteristics of the Princeton Sailwing concept. The results of experiments with several models are presented and conclusions drawn which generally compare the sailwing to a conventional wing of similar planform geometry.

This report describes the structure and the dominant aerodynamic characteristics of the Princeton Sailwing concept. The results of experiments with several models are presented and conclusions drawn which generally compare the sailwing to a conventional wing of similar planform geometry.

AD _____	Accession No. _____	UNCLASSIFIED	AD _____	Accession No. _____	UNCLASSIFIED
Princeton University Aero. Eng. Dept., Princeton, N. J.		1. Sailwing structure 2. Sailwing wind tunnel tests 3. Sailwing Free Flight models 4. Navion wing wind tunnel tests 5. Sailwing man- carrying machine 6. T. E. Sweeney 7. Contract No. DA44-177-TC-524	Princeton University Aero. Eng. Dept., Princeton, N. J.		1. Sailwing structure 2. Sailwing wind tunnel tests 3. Sailwing Free Flight models 4. Navion wing wind tunnel tests 5. Sailwing man- carrying machine 6. T. E. Sweeney 7. Contract No. DA44-177-TC-524
EXPLOATORY SAILWING RESEARCH AT PRINCETON - T. E. Sweeney			EXPLOATORY SAILWING RESEARCH AT PRINCETON - T. E. Sweeney		
Report No. 578, December, 1961 35 pp.			Report No. 578, December, 1961 35 pp.		
Contract No. DA44-177-TC-524 Project No. 9-38-10-000, TK902 Unclassified Report			Contract No. DA44-177-TC-524 Project No. 9-38-10-000, TK902 Unclassified Report		